Proceedings of 2nd International Conference on Mechanical and Aeronautical Engineering
Held on 13th – 14th July 2016, in Bangkok, ISBN: 9788193137352

INVESTIGATION AND GENERALIZATION OF CONVECTIVE HEAT TRANSFER IN DIFFERENT ROOM GEOMETRIES

O. Acikgoz,
Heat and Thermodynamics Division,
Department of Mechanical Engineering,
Yildiz Technical University, Yildiz, Besiktas,
Istanbul, 34349, Turkey

A.S. Dalkilic,
Heat and Thermodynamics Division,
Department of Mechanical Engineering,
Yildiz Technical University, Yildiz, Besiktas,
Istanbul, 34349, Turkey

S. Wongwises
Fluid Mechanics, Thermal Engineering and Multiphase
Flow Research Lab. (FUTURE), Department of Mechanical Engineering,
King Mongkut's University of Technology Thonburi,
Bangmod, Bangkok 10140, Thailand

Abstract- In this numerical case study, modeled enclosures of different floor areas at a constant height (2.85 m) are heated from one wall and cooled from the opposite wall to make an actual room model. The cooled wall simulates the heat loss of the room, and the heated wall simulates the heat source of an enclosure. The convective heat transfer that occurs during this process is studied numerically within two- (2D) and three-dimensional (3D) models. Various wall temperatures (T_h= 20-35°C; T_c=5-15°C) and floor areas (L×L= 1.8 × 1.8 m; 4.0 × 4.0 m; 6.0 × 6.0 m) are assigned to derive equations that contain characteristic length (L) in Rayleigh number. Conclusions have been compared with the results of correlations that were formerly explored and suggested for enclosures in the literature. Furthermore, new correlations for the average Nusselt number in enclosures within definite Rayleigh-number intervals (maximum 3.08 × 109≤RaL≤6.59 × 1011), as well as aspect ratios (0.48≤H/L≤1.58), are found.

Keywords- Convective heat transfer, Convection correlations, Nusselt number, Enclosures

I. Introduction

Lowering energy consumption and improving thermal comfort are the most significant purposes of building engineering. According to many researchers' studies, different usages of convective heat transfer coefficient (CHTC) correlations in heating system simulations have considerable impact on calculated heating load in buildings. Hence, the correct utilization of CHTCs in real-size room enclosures carries utmost importance for both energy consumption and thermal comfort. Even though conduction and radiation heat transfer simulation models in actual-sized rooms were comprehensively investigated by many scholars, some uncertainties still exist in convection. Problems exist with exact convection modeling, particularly by means of analytical and numerical approaches caused by the difficulty of the enclosure shape, clarification of fluid dynamics problems (governing equations), and alterations at each air flow sample in each heating preference.

Because of their significance in industry and living residences, natural convection, temperature, and velocity distribution problems in enclosures are broadly examined in enclosures, usually experimentally but also numerically. Presently, the heating systems of vertical walls are not used much, but with development of renewable energy methods and low temperature heating systems, their usage will widen. In this context, determining CHTCs in enclosures heated from walls will be much more important. In order to calculate CHTCs and Nusselt numbers, CFD codes have been used in this study.

ASHRAE [1] has listed many convective heat transfer coefficient values and correlations. Nevertheless, these equations have been explored with the assumption that CHTC in an enclosure tends to have similar behavior with free-edge insulated plates. However, air flow at surrounding walls, even though they are not heated or cooled, affects the flows on adjacent walls. In addition, air flows over all surfaces affect the flow pattern in the whole enclosure. Consequently, equations derived for free plates cannot be exactly employed for free convection problems in enclosures. [2]. It can also be stated that CHTC correlations derived through 2D infrastructure for an enclosure cannot be relied on, since contiguous wall influences that are omitted from numerical procedures or analytical expressions. Moreover, experimental and numerical studies point out that CHTCs of actual room surfaces are influenced by the depth or height of the room, the boundary conditions of the surface, the smoothness/roughness of surfaces, and whether forced convection exists in the room.

Peeters et al. [2] had a comprehensive review on experimentally obtained CHTCs in enclosures and over free plates. They sorted these correlations in relation to heating preferences, flow intensity, and reference temperature preference in the enclosure. In addition, they examined the accuracy of the equations obtained by many scientists and conducted novel experiments to confirm equations. Large differences were found among current equations in open sources. The alterations have been explained by the values of estimated coefficients, the reference air temperatures selected, and the formats of the equations. They asserted that the determination and selection of proper characteristic length carries great importance as well.
In his study, Beausoleil-Morrison [3] showed the influence of CHTC equations on building heating load evaluations. He carried out experimental work in appropriately isolated sample structures that contained radiant heating systems. Simulations benefitting from many CHTC correlations and measurements through test buildings found 8% difference. He also deduced that building load rates were more sensitive to tested CHTC equations and the adjusted set point of the room than building fabric, thermal goods, and air infiltration.
Fohonno and Polidori [4] have proposed analytic model of convective heat transfer between an isolated vertical plate and natural convective flow. They supposed a constant heat flux on a surface, and the model they developed permitted mean and local CHTCs to be determined in laminar and turbulent flow. The equation they obtained for mean CHTC was derived through local CHTC results, and this provided a transition from laminar to turbulent regions and counted the height of the plate in the correlation. They stated that a good agreement was seen between Alamdari and Hammond's correlation. The new correlation's validity to actual-size rooms were taken into account, and in spite of the three dimensionality of actual-size rooms, there was a 10% difference between data taken through the experimental chamber.

Awbi and Hatton [5] investigated free convection in two different enclosures. The enclosures' sizes were 2.78 mby 2.30 m by 2.78 m and 1.05 m by 1.01 m by 1.05 m. One of the enclosures' walls was used as a "heat sink" via an air conditioner located in a small room beside the large enclosure. The walls opposite and adjacent to the "heat sink" wall have been heated with impregnated flexible sheets that have a 200 W/m2 output. Thermocouples were placed inside and outside the surfaces. Reference air temperature for the wall heating system has been taken 100 mm from the heated surface and designated as "undisturbed air temperature", in other words, the temperature outside thermal boundary layer. Consequently, the temperature difference variances in CHTC and Nusselt number correlations were determined as temperature difference between surface and undisturbed air temperature. Thermal radiation was found by using the measured emissivity of the surfaces and derived from total heat flux. Since they also partly heated the walls, characteristic length was calculated as hydraulic diameter. The outcomes presented were interpreted and stated that CHTC's for a heated wall were lower than found in the small enclosure that has

Table 1 Correlations derived for CHTC and Nusselt number in enclosures

Correlation	Conditions	Reference temperature
Awbi and Hatton		
$h = \frac{1.823}{D^{0.121}}(\Delta T)^{0.293}$ $Nu = 0.289(Gr)^{0.293}$	Heated wall (2.78x2.30x2.78 m)	Local air temperature (100 mm from wall)

Khalifa and Marshall		
$h = 2.30(\Delta T)^{0.24}$	For a room with a heated wall and a room heated by a radiator under a window. (2.35x2.95x2.08 m)	Average room temperature
$h = 2.10(\Delta T)^{0.23}$	For a room heated by a fan heater. (2.35x2.95x2.08 m)	Average room temperature
ASHRAE		
$Nu = 0.117(Gr)^{0.117}$	Turbulent flow 10^8<Gr<10^{12}	Average room temperature
Li et al.		
$h = 3.08(\Delta T)^{0.25}$	Normal conditions, occupied room.	Average room temperature
Min. et al.		
$h = 1.646\frac{(\Delta T)^{0.32}}{H^{0.05}}$	Heated floor or heated ceiling	Average room temperature

Table 2 Hot surface Nusselt numbers at different meshing numbers
(LxHxL= 1.8 x 2.85 x 1.8 m; 2-D model's results, T_H= 30°C, T_C= 10°C, other walls are kept adiabatic)

Interval count at x and y axes	Surface Average Nusselt number
30 x 25	308.57
60 x 50	331.83
120 x 100	343.24
240 x 120	348.81

Table 3 Hot surface Nusselt numbers at different meshing numbers for the same conditions in Table 2

Interval count at x, y and z axes	Surface Average Nusselt number
20 x 15 x10	278.06
30 x 30 x 10	290.57
45 x 40 x 20	309.66
60 x 50 x30	315.22

approximately 1 m3 volume. However, in order to evaluate if the difference was because of the heating plate sizes or enclosure sizes, more experiments were performed with small plates placed on surfaces. It has been seen that there is a close agreement between CHTCs determined with whole wall heated experiments and small plates heated experiments. As a result, they stated that rather than the heated area on a wall, size of the enclosure considerably influences CHTC. They did comparison with their results with those from the equations in open sources and their data were determined in the central of the curves. Correlations they suggest for walls as well as the derived by other researchers can be seen in Table 1.

Awbi [6] has revealed the outputs of a CFD work regarding convective heat transfer coefficients of a heated wall, a heated floor, and a heated ceiling. He benefitted from two turbulence models: standard k-ε model using wall functions and low Reynolds k-ε model. The outputs have been compared with experimentally found data.

To calculate CHTCs for entire surfaces in an enclosure Khalifa and Marshall [7] have set up an experimental chamber that has dimensions parallel with actual size room of a building. 65 aluminum thermistors were places in order to determine air and surface temperatures in the enclosure. Inner and outer surfaces of the chamber were covered with aluminum. Radiant heat exchange were not counted in the CHTC calculation process. Additionally, an uncertainty analysis was conducted. Temperature measurements, conductivity of the materials and the lack of inclusion of long wave radiation in the low emissivity chamber have been taken into account during uncertainty analysis [2]. They proposed various equations, two of them have been incorporated in Table 1.

Khalifa [8] prepared a comprehensive review of two- and three-dimensional free convection, concentrating mainly on heat transfer in buildings. He indicated that the discrepancies are about up to a factor of 5 for vertical surfaces, 4 for horizontal surfaces facing upward, and up to 8 for horizontal-facing downward surfaces.

Khalifa and Khudheyer [9] have carried out an experimental study on the influences of 14 dissimilar configurations of partitions on free convection heat transfer in enclosures. Similar to investigations in open sources, the experiment reflected vertical hot and cold walls, while the other walls were isolated. The study has been done within the Rayleigh numbers ranges of 6.107- 1.5.108, along with the aspect ratio of 0.5. Equations that are accurate for the experimental works have been explored.

Khalifa [10] did a broad review of investigations on insulated vertical and horizontal surfaces. Evaluations between equations for heat transfer coefficients were realized, and the discrepancies were calculated to be up to a factor of 2 for isolated vertical surfaces, up to a factor of 4 for isolated horizontal surfaces facing upward, and up to 4 for isolated horizontal surfaces facing downward.

Assaf et al. [8] found a new method to design the dry-expansion shell and U-tube evaporators. They used Modelica language which provides a model with a general flow arrangement. The authors validated the model using a commonly seen shell and tube evaporator employed with R134a. Pure R134a, R407C and a special chosen glide matching refrigerant were flowed. As result, it was seen that the influence of temperature profile of refrigerant mixtures can be considerable on the relative performance of a specific heat exchanger configuration.

Abed et al. [9] reviewed the improvement techniques as well as falling film flow, particularly the impact of nanoparticles that took place in refrigerants.The review study also includeseffect of geometry of surfaces, low fins, developed geometrical tubes and problems on refrigerant-based nanofluids. It has been concluded that the interaction between heat and mass transfer on falling film flow and disagreements of thermal properties of nanofluids should be regarded as well. As result, the study shed light on the factors that influence effectiveness, compactness and cost of spray evaporators as well as available improvement methods.

Hosseini et al. [10] experimentally investigated the heat transfer coefficient and pressure drop on the shell side of a shell and tube heat exchanger for different types of copper pipes. Novel correlations for both pressure drop and Nusselt number were explored valid for different tube types (smooth, corrugated, and with microfin). The tube groups that have the identical geometric and structural arrangements except different external tube surfaces inside the shell were utilized for the experimental work. In conclusion, corrugated and micro-fin tubes have revealed deterioration of efficiency at a Reynolds number field (Re < 400). Also, at a greater Reynolds number for micro-finned tubes the effectiveness of the heat exchanger has shown considerable enhancement.

In the work, which may be evaluated as the first experimental study for CHTCs in enclosures, Min et al. [11] investi gated within the range of Rayleigh number 109 to 1011 and with enclosure dimensions 3.60 by 7.35 by 2.40 m, 3.60 by 7.35 by 3.60 m, and 3.60 by 3.60 by 2.40 m, and presented equations for CHTCs. These equations were proposed for non-ventilated conditions. Unheated surfaces were kept at constant temperature. Temperatures of the surfaces and the heat fluxes given to the enclosure were determined. Radiation influences were regarded as well, whereas the temperatures of the surfaces that were not heated varied between 4.4oC-21.1oC, the temperatures of the floor surfaces changed between 24oC-43.3oC, and the temperature of the ceiling surface changed between the ranges of 32.2oC-65.6oC.

By means of numerical methods, Karadağ [12] has examined the correlation between radiative and convective heat transfer coefficients for ceilings when the floor surface is insulated. To reach this purpose, he initially neglected the radiative heat transfer at the surfaces ($\varepsilon w = \varepsilon c = 0$) at different room dimensions (3 by 3 by 3 m, 4 by 3 by 4 m, and 6 by 3 by 4 m) and thermal boundary conditions (Tc = 0 - 25oC, Tw = 28 - 36oC). At that point, Karadağ determined the radiative heat transfer for distinct surface emissivities ($\varepsilon w = \varepsilon c$=0.7-0.8 and 0.9). The numerical outputs that were obtained were evaluated with outputs in open sources.

The ratios of radiative heat transfer to convective heat transfer coefficients were determined, and it was seen that the ratios changed from 0.7 to 2.3.

Karadağ et al. [13] numerically examined the alteration of Nusselt number with ceiling and floor temperatures and room sizes. The wall temperatures were kept at constant and the ceiling temperature was varied from 10 to 25oC at various room dimensions. It has been seen that when the temperature between the ceiling and air was raised, the Nusselt number over the floor also increased. Correlations in the literature that do not take into account the ceiling and floor temperatures deviate up to 35% from the real data. Consequently, it has been stated that a new equation for the Nusselt number over the floor that encompasses the effect of thermal conditions and all room sizes should be explored.

Li et al. [14] studied free convection in an occupied office room under usual working circumstances equal to a temperature difference of 1.5°C.

Davies et al. [15] carried out a project to enable accurate measurement of convective heat transfer coefficients in real buildings. The tests were realized by measuring the convective heat transfer coefficients on a heated plate that was placed in a test room. The results showed that the difference between the results of this new instrument and the classic heated plate method was small. Their new method has the potential to be used in real buildings.

Although many laminar regime natural convection problems in an enclosure have been solved in the literature, the turbulent free convection problem in an enclosure of an approximate size as an actual room size that is heated from one wall and cooled from the opposite wall has not been rigorously investigated by means of computation, particularly by reason of the length of the solution periods. The major aim of this work is to examine two and three dimensionally the effect of hot and cold wall temperatures of the enclosure and characteristic length on the average Nusselt number and the CHTC in enclosures by means of computational methods. Afterwards, the gained data has been compared with the equations in open sources, given in Table 1. This study should be acknowledged as a continuation of the authors' formerly published work [19]. In addition to the authors' previous paper [19], the research has been conducted in smaller as well as larger geometries in order to widen the Rayleigh number range and accurately derive correlations in a broad range; this approach has also enabled the study to be at different aspect ratios (H/L). Hence, as an enhancement to the correlations in the previous studies, the aspect ratio (H/L) has been incorporated into the Nusselt number correlations that are valid within a broader interval ($3.08x10^9 \leq Ra_L \leq 6.59x10^{11}$). Also, the brief information on the new findings can be seen from the authors 'other publication [20].

I. Numerical model

Due to the fact that the solution of related equations in large geometries such as the case studies of this work last substantially long periods, the usage of computational fluid dynamics (CFD) programs was not so convenient until recent years. On the other hand, developing computer knowhow today permits engineers to use CFD programs in engineering applications. The frequent mesh density in the boundary layers of the model of the room CFD software enable outputs in tolerable periods, mainly in two- and three-dimensional solutions. In the present work, we have employed numerical techniques to determine the mean Nusselt number and CHTC over the heated wall of an enclosure, which has similar sizes with the room of a building. A three-dimensional natural convection problem in an enclosure with the dimensions of 1.80 by 2.85 by 1.80 m, 4.00 by 2.85 by 4.00, and 6.00 by 2.85 by 6.00 were considered, while 2.85 m were kept constant in order to resemble a real room height and floor area that was varied from 1.80 x 1.80 to 6.00 x 6.00. In order to obtain the approximate wall temperatures with wall heating systems, the heated sidewall was heated within the range of 20°C to 35°C, while the cooled wall that served as a heat sink was cooled from 5°C to 15°C. The other faces of the enclosure have been kept adiabatic.

The greatest noteworthy front of solving a problem through CFD software is to design and favorably mesh the enclosure. To obtain 2-D and 3-D designs of the enclosure, GAMBIT 2.4.6, a designing and meshing program, was preferred. In basic geometries, as in the current work model, the quad/hex meshes enable more reliable solutions with less cells than a tri/tet mesh. Therefore, the whole surface of the enclosure was selected as plane quad/hex meshes in current work. To reduce the meshing influences on the outputs in each modeling types, two- and three-dimensional edges of both 2-D and 3-D designed rooms have been meshed with various interval counts. In order to detect if the mesh influence has been sufficiently reduced, the Nusselt numbers were obtained from FLUENT for each modeling case. As the difference between last two solutions is so slight, the interval count before the last one (120x100) has been chosen as the appropriate number, as can be seen in Table 2. In other words, the distance between heated

and cooled walls (characteristic length) was divided into 120 intervals. These intervals were chosen to be frequent near walls by reason of the quick temperature differences in the surface boundary layers, while the intervals were determined to be less frequent toward the center of the model (Figs. 1-2).The temperature variation from the outside of the boundary layer to the center of the room is nearly zero, as is shown in Fig. 3. To take this into account, the "first length" option in the program, the ratio of mid-point interval size at the edge to the first interval size at the corner of the edge was chosen as 0.001. Although the height of the enclosure (2.85 m) was longer than the characteristic length (1,80 m), it was divided into 100 intervals since most of the heat transfer has occurred between these walls. Also, in 2-D and 3-D solutions, similar to the above-mentioned procedures, discrete interval counts on two and three axes have been executed and a suitable interval count was found to be 120 x 100 and 45 x 40 x 20, as can be seen in Tables 2 and 3, respectively. In addition, air has been selected as the fluid that exists in the enclosure.

The FLUENT 6.3 program, one of the commonly used codes have been employed to solve related equations

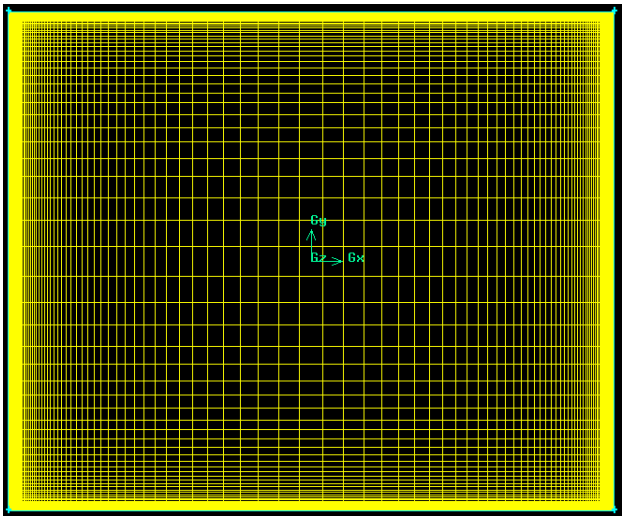

Fig. 1 Meshing (x-y) detail of two dimensional room (L x H= 1.8 m x 2.85 m)

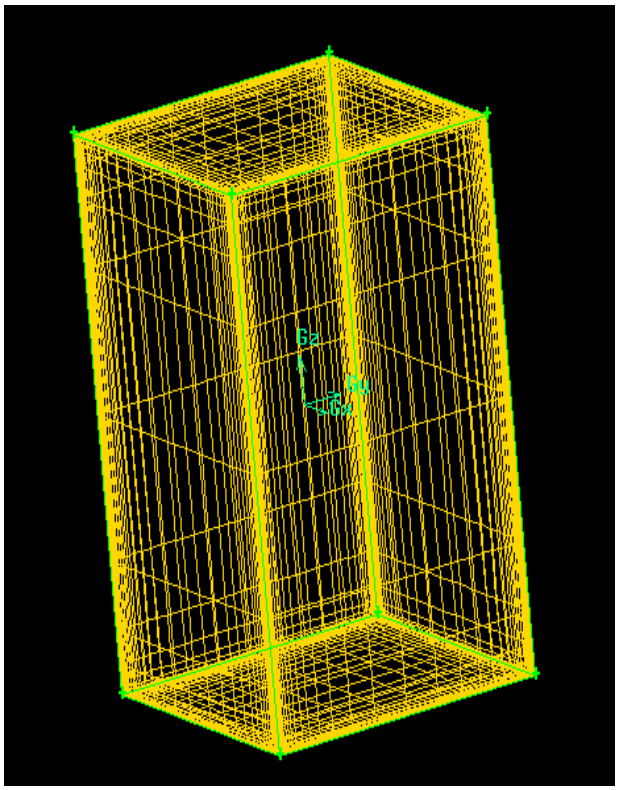

Fig. 2 Meshing detail of three dimensional room (LxHxL= 1.8 m x 2.85 m x 1.8 m)

(energy, momentum, continuity, and turbulence). The frame of the software's solution techniques is based on the control volume theory as converting related equations into algebraic equations to deal with them. The control volume techniques are driven by conducting the integration of the governing equations on the individual control volume and generating discretization of the equations [16]. In the model, the key dimension used is characteristic length (L=1.8 m, 4.0 m, 6.0 m), the difference between heated and cooled walls (i.e., opposite walls). Along with characteristic length, the Rayleigh numbers for the system have been determined; one example can be seen in Eq. [10] and full Rayleigh numbers are presented in Tables 4 and 5.

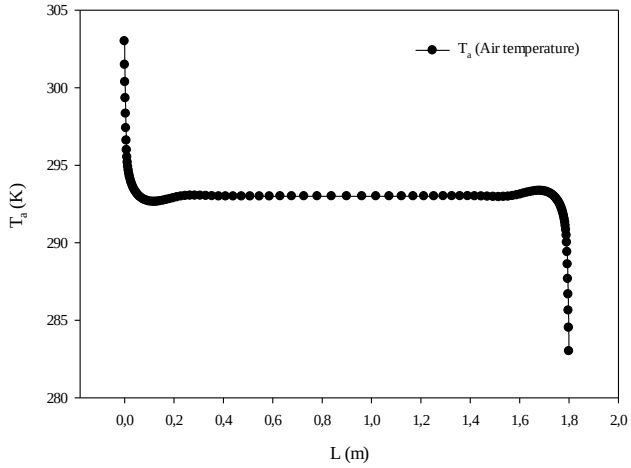

Fig. 3 Temperature variation along the center of enclosure, from mid-point of the hot wall to the cold wall

As the whole calculated Rayleigh numbers were larger than 109, a turbulence model was employed in the flow pattern. The first order upwind scheme was operated to discrete governing equations. The under relaxation factors for density, momentum, turbulence kinetic energy, turbulence dissipation rate, turbulent viscosity, and energy (1.0, 2.0, 0.8, 0.8, 1, and 0.9) have been chosen to converge at the solution. The case studies were done by a notebook which has an Intel Core i5 processor 2430M CPU, 2.40-GHz, 6-GB Ram Windows 7 Home Basic 64-Bit SP1 operating system. Further, the required solution period for each appropriate (i.e., meshing effect minimized) case has lasted approximately 12 hours.

The related equations for the turbulence 3-D flow is shown as:

Continuity equation:

$$\frac{\partial u}{\partial x}+\frac{\partial v}{\partial y}+\frac{\partial w}{\partial z}=0 \tag{1}$$

Momentum equations:

$$\rho\left(u\frac{\partial u}{\partial x}+v\frac{\partial u}{\partial y}+w\frac{\partial u}{\partial z}\right)=-\frac{\partial p}{\partial x}+\mu\left(\frac{\partial^2 u}{\partial x^2}+\frac{\partial^2 u}{\partial y^2}+\frac{\partial^2 u}{\partial z^2}\right) \tag{2}$$

$$\rho\left(u\frac{\partial v}{\partial x}+v\frac{\partial v}{\partial y}+w\frac{\partial w}{\partial z}\right)=-\frac{\partial p}{\partial x}+\mu\left(\frac{\partial^2 v}{\partial x^2}+\frac{\partial^2 v}{\partial y^2}+\frac{\partial^2 v}{\partial z^2}\right) \tag{3}$$

$$\rho\left(u\frac{\partial v}{\partial x}+v\frac{\partial v}{\partial y}+w\frac{\partial w}{\partial z}\right)=-\frac{\partial p}{\partial x}+\mu\left(\frac{\partial^2 v}{\partial x^2}+\frac{\partial^2 v}{\partial y^2}+\frac{\partial^2 v}{\partial z^2}\right) \tag{4}$$

Energy equation:

$$\rho\left(u\frac{\partial T}{\partial x}+v\frac{\partial T}{\partial y}+w\frac{\partial T}{\partial z}\right)=\alpha\left(\frac{\partial^2 T}{\partial x^2}+\frac{\partial^2 T}{\partial y^2}+\frac{\partial^2 T}{\partial z^2}\right) \tag{5}$$

The residual values were chosen as 10^{-6} for energy and 10^{-3} for momentum and continuity equations. The physical properties of air (thermal conductivity, specific heat, density, and viscosity) in the room have been entered into the program as the mean temperature value of hot and cold walls from Incropera and DeWitt 's [16] physical properties of air specifications.

FLUENT performs two different solver types "pressure based" and "density based." In the current work, we have chosen the "density-based" and Boussinesq approach. Among various viscous models presented by the program, as suggested by Karadag et al. [13], "k-ε" was chosen, and the model of "k-ε" was selected as the "standard" that was employed by Awbi [6] as well. Works in open sources advice that the k-ε standard model is the most suitable solution model for free convection. The most commonly used engineering turbulence model for industrial applications, it is strong, tolerably precise, and covers submodels for compressibility, buoyancy, and combustion, etc.

Moreover, it is favorable for first iterations, as well as the first screening of alternative models and parametric works, such as this study [17]. The turbulence kinetic energy, k, and the dissipation rate, ε, have been determined through the transport equations [8] and [9], respectively:

$$\frac{\partial}{\partial x}(\rho k u)=\frac{\partial}{\partial y}\left(\left[\left(\mu+\frac{\mu_t}{\sigma_k}\right)\frac{\partial k}{\partial y}\right]\right)+G_k-\rho\varepsilon \tag{6}$$

$$\frac{\partial}{\partial x}(\rho\varepsilon u)=\frac{\partial}{\partial y}\left(\left[\left(\mu+\frac{\mu_t}{\sigma_\varepsilon}\right)\frac{\partial \varepsilon}{\partial y}\right]\right)+C_{1\varepsilon}\frac{\varepsilon}{k}G_k-\rho C_{2\varepsilon}\frac{\varepsilon^2}{k} \tag{7}$$

while

Table 4 Change of Nusselt numbers and CHTC's at various wall temperature and room dimensions (2-D model results)

	180*285*180 T_C=5°C			**400*285*400 T_c=5°C**			**600*285*600 T_c=5°C**		
T_h(°C)	**Ra**	**Nu**	**h**	**Ra**	**Nu**	**h**	**Ra**	**Nu**	**h**
20	1.00E+10	327.82	4.58	11E+11	721.52	4.53	3.7E+11	1075.88	4.5
25	1.28E+10	355.92	5.01	1.41E+11	783.07	4.96	4.75E+11	1167.94	4.93
30	1.54E+10	378.01	5.36	1.69E+11	832.38	5.31	5.71E+11	1241.71	5.28
35	1.78E+10	395.83	5.65	1.95E+11	870.14	5.59	6.59E+11	1299.54	5.57
	180*285*180 T_C=10°C			**400*285*400 T_c=10°C**			**600*285*600 T_c=10°C**		
T_h(°C)	**Ra**	**Nu**	**H**	**Ra**	**Nu**	**h**	**Ra**	**Nu**	**H**
20	6.41E+09	277.3	3.9	7.03E+10	614.2	3.88	2.37E+11	914.78	3.86
25	9.24E+09	316.15	4.48	1.01E+11	695.23	4.43	3.42E+11	1035.79	4.41
30	1.19E+10	343.24	4.9	1.3E+11	754.31	4.85	4.39E+11	1126.11	4.82
35	1.43E+10	364.45	5.24	1.57E+11	801.39	5.2	5.28E+11	1196.28	5.16
	180*285*180 T_C= 15°C			**400*285*400 T_c= 15°C**			**600*285*600 T_c=15°C**		
T_h(°C)	**Ra**	**Nu**	**H**	**Ra**	**Nu**	**h**	**Ra**	**Nu**	**H**
20	3.08E+09	215.2	3.05	3.38E+10	472.16	3.01	1.14E+11	703.02	2.99
25	5.93E+09	269.66	3.85	6.51E+10	590.85	3.8	2.2E+11	881.14	3.77
30	8.56E+09	304.72	4.38	9.39E+10	669.71	4.34	3.17E+11	998.44	4.31
35	1.10E+10	330.64	4.8	1.21E+11	727.26	4.75	4.07E+11	1084.63	4.72

Table 5 Change of Nusselt numbers and CHTC's at various wall temperature and room dimensions (3-D model's results)

180*285*180 T_C=5				**400*285*400 T_C=5**			**600*285*600 T_C=5**		
T_h	**Ra**	**Nu**	**h**	**Ra**	**Nu**	**h**	**Ra**	**Nu**	**h**
20	1.00E+10	296.03	4,13	1.1E+11	647.11	4.06	3.7E+11	962.88	4.03
25	1.28E+10	321.5	4,52	1.41E+11	703.08	4.44	4.75E+11	1046.36	4.41
30	1.54E+10	341.49	4,84	1.69E+11	747	4.76	5.71E+11	1111.88	4.73
35	1.78E+10	355.29	5,07	1.95E+11	781.9	5.02	6.59E+11	1163.95	4.99
	180*285*180 T_C=10			**400*285*400 T_C=10**			**600*285*600 T_C=10**		
T_h	**Ra**	**Nu**	**h**	**Ra**	**Nu**	**h**	**Ra**	**Nu**	**h**
20	6.41E+09	252.07	3,54	7.03E+10	550.66	3.48	2.37E+11	819.05	3.45
25	9.24E+09	285.43	4,04	1.01E+11	623.9	3.98	3.42E+11	928.27	3.95
30	1.19E+10	309.66	4,42	1.3E+11	677.82	4.35	4.39E+11	1007.67	4.32
35	1.43E+10	329.23	4,74	1.57E+11	720.13	4.66	5.28E+11	1071.84	4.63
	180*285*180 T_C= 15			**400*285*400 T_C= 15**			**600*285*600 T_C= 15**		
T_h	**Ra**	**Nu**	**h**	**Ra**	**Nu**	**h**	**Ra**	**Nu**	**H**
20	3.08E+09	194.15	2,75	3.38E+10	423.68	2.7	1.14E+11	629.87	2.68
25	5.93E+09	242.98	3,47	6.51E+10	530.78	3.41	2.2E+11	789.45	3.38
30	8.56E+09	275.13	3,96	9.39E+10	601.35	3.89	3.17E+11	894.66	3.86

35	1.10E+10	298.77	4,33	1.21E+11	653.27	4.26	4.07E+11	972.13	4.23

$$\mu_t = \rho c_p \frac{k^2}{\varepsilon} \quad (8)$$

$$G_k = -\rho \overline{\upsilon' u} \frac{\partial \upsilon}{\partial x} \quad (9)$$

where $C_{1\varepsilon}$ and $C_{2\varepsilon}$ are constants and σ_k and σ_ε are the turbulent Pr numbers for k and ε, in turn. Also, the k-ε model constants, C_μ, $C_{\varepsilon 1}$, $C_{\varepsilon 2}$, σ_k, σ_ε, are equal to 0.09, 1.44, 1.92, 1.0, and 1.3, respectively [17, 18].

Since the purpose of the study is to obtain the average CHTC in the enclosure and the program yields, including the surface radiation heat transfer coefficient in CHTC and could not be distinguished from each other, no radiation model has been employed from among the "Models" part of the software. Thus, only CHTC in the enclosure has been found.

In FLUENT, the thermal boundary conditions can be stated with five different methods: constant heat flux, constant temperature, convection, radiation, and mixed. In this current work, the wall surfaces except those that are heated and cooled were assigned as adiabatic and given as "0 W/m^2" to have adiabatic boundary conditions in the program. In addition, the thermal boundary conditions of the heated and cooled walls that stand opposite were defined as the constant temperature.

According to a previously published work by Karadag et al. [13], Nusselt numbers have been determined as a reference to determine whether or not the meshing influence on the outputs was reduced. For validating the results taken through the program, the results in Table 4 were validated by making them equal to the conduction heat transfer in the boundary layer to the convective heat transfer outside this zone, thus verifying the equality.

While the hot wall temperature is calculated through the program's "area weighted surface temperature" specialty, β, α, and γ are determined at the film temperature; in other words, the mean temperature of hot and cold wall temperatures. If we calculate the Rayleigh number for the 1.8 by 2.85 by 1.8 m room that can be seen in Figs. 1 and 2 when the hot and cold wall temperatures are 30°C and 10°C, respectively, it should be noted that the Rayleigh number is above 109 and, as a result, the flow pattern in the room is turbulent, while the characteristic length is the distance between hot and cold walls.

$$Ra = \frac{g\beta L^3 (T_H - T_C)}{\gamma \alpha} \quad (10)$$

$$Ra = \frac{9{,}81.0{,}0034.1{,}8^3.(30-10)}{15{,}26.10^{-5}.2{,}15.10^{-5}} = 1{,}19.10^{10} \rangle 10^9$$

(turbulent flow)

All of the obtained Rayleigh numbers at various wall temperatures and room-floor surface dimensions have been presented in Tables 4 and 5. The Nusselt numbers and CHTCs at corresponding Rayleigh numbers can be seen in these tables as well. The proportional difference between the last two surface Nusselt numbers is about 1%, and this means that the meshing effect on the results have been substantially dispelled (Tables 2 through 3).

Figs. 1 and 2 show the meshing detail of the 2-D and 3-D room, respectively, while meshes become frequent near the edges because of the boundary layer effects. Fig. 3 illustrates the temperature alteration along the horizontal center of the enclosure, from the midpoint of the hot wall to the midpoint of the cold wall.

II. Results and Discussion

Numerical studies have been executed in relation to the steps that were explained above in the "Numerical Model" section. In these studies, various hot and cold wall temperatures and characteristic lengths have been employed so as to attain several points on the Nusselt-Rayleigh number diagrams. Figs. 4 through 6 illustrate the alteration of the hot wall surface mean Nusselt number with variations of cold wall temperatures for three room dimensions for both 2-D and 3-D. As it can be seen from the trend lines on the figures, Nusselt number increases with increasing Rayleigh numbers.

As also can be seen in Tables 4 and 5, fairly accurate differences between these outputs is 10%. It is obvious from the figures that while the cold wall temperature increases, the temperature difference between the hot wall and the cold wall decreases and, therefore, the Nusselt number over the hot wall also decreases. It can, hence, be indicated that the temperature of the cold wall in a room influences the Nusselt number and the CHTC in the enclosure. Figs. 7 through 9 show the change of the average Nusselt number with the Rayleigh number at different cold wall temperatures (5-15°C) for several room dimensions (1.80 by 2.85 by 1.80 m, 4.00 by 2.85 by 4.00 m,and 6.00 by 2.85 by

6.00 m). Through these figures, the change of the Nusselt number with the Rayleigh number over the heated wall at constant cooled wall temperatures (5-15°C) in real size enclosures that have different floor areas are observed. It can easily be seen that, as the characteristic length increases, the Nusselt number over the hot wall increases as well.

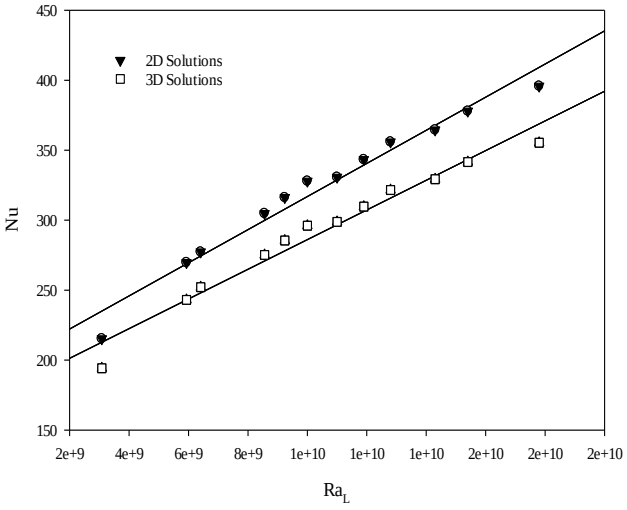

Fig. 4 Change of Nusselt number with Rayleigh number for different wall temperatures (LxHxL= 1.8 x 2.85 x 1.8 m; T_c=5-15°C, T_H= 20-35°C)

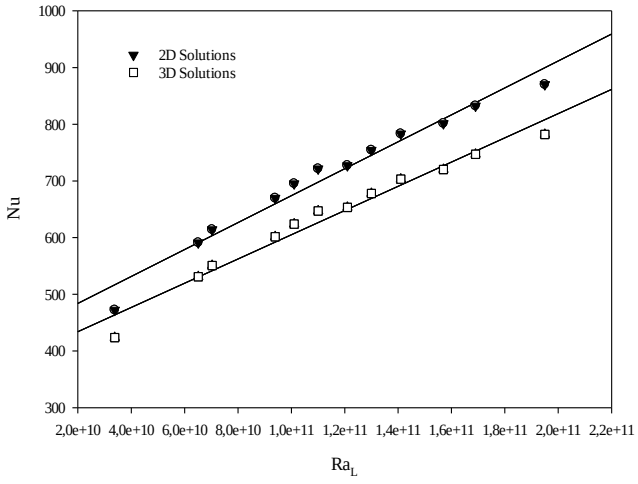

Fig. 5 Change of Nusselt number with Rayleigh number for different wall temperatures (LxHxL= 4.0 x 2.85 x 4.0 m; T_c=5-15°C, T_H= 20-35°C)

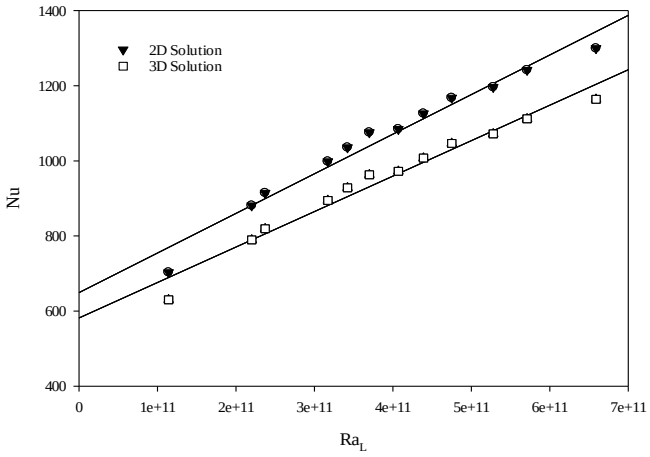

Fig. 6 Change of Nusselt number with Rayleigh number for different wall temperatures (LxHxL= 6.0 x 2.85 x 6.0 m; T_c=5-15°C, T_H= 20-35°C)

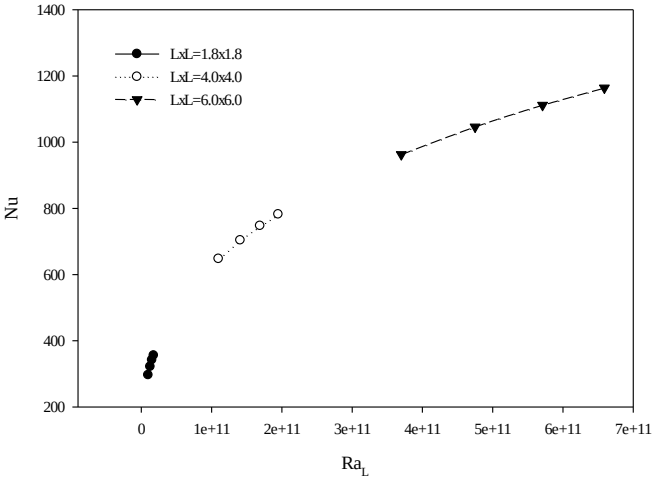

Fig. 7 Change of Nusselt number with Rayleigh number for different floor dimensions (H= 2.85 m, T_c=5°C, T_H= 20-35°C)

Figs. 10 through 12 present the variation of the CHTC at different floor areas and a constant enclosure height (LxL= 1.8x1.8 m, 4x4 m, 6x6 m), (H= 2.85 m). The results obtained at each floor area have been compared with the correlations explored by other researchers that can also be seen in Tables 4 and 5. The results of the 3-D solutions stand in the middle of the curves. The trend lines on all (h-ΔT) figures in the paper indicate that CHTC increases with increasing temperature differences.

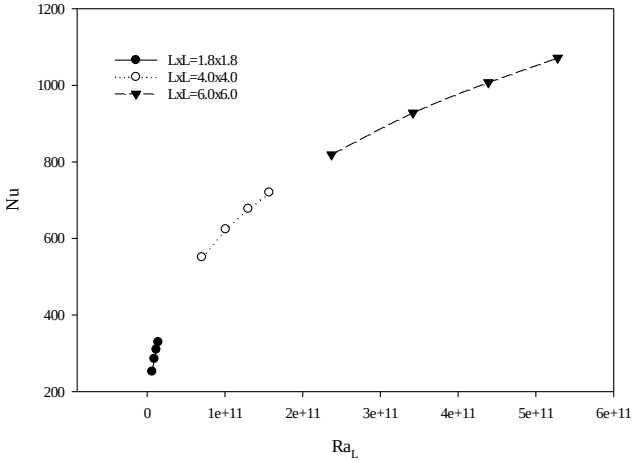

Fig. 8 Change of Nusselt number with Rayleigh number for different floor dimensions (H= 2.85 m, T_c=10°C, T_H= 20-35°C)

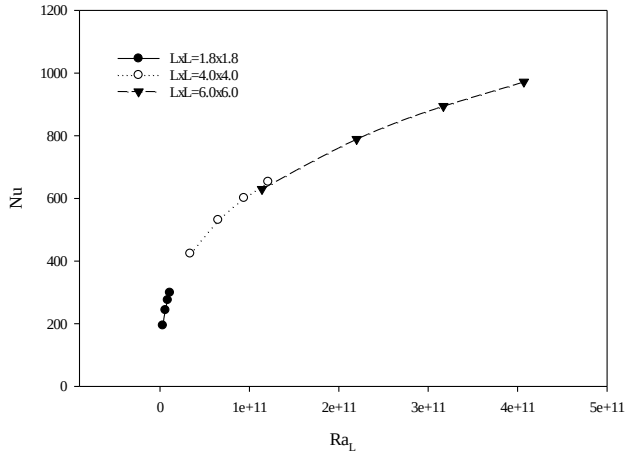

Fig. 9 Change of Nusselt number with Rayleigh number for different floor dimensions (H= 2.85 m, T_c=15°C, T_H= 20-35°C)

In Fig. 13, the results of this numerical study, which were implemented using FLUENT for proper hot and cold wall temperatures parallel with actual wall temperatures in buildings hot and cold wall temperatures for actual room surfaces and room dimensions were evaluated with the outputs of correlations given in open sources.

For whole Rayleigh numbers, which are shown in Tables 4 and 5, the Nusselt numbers corresponding to these numbers were taken by using the software and are shown in Figure 13. It can be deduced that, as well as the Rayleigh number, the Nusselt number depends on hot and cold wall temperatures and room sizes. In relation to all of these acquired numbers and Fig. 13, we have obtained four new Nusselt number correlations for an enclosure similar to an actual room dimension of a building within the maximum Rayleigh number range of $3.08x10^9$ to $6.59x10^{11}$, while the temperature difference variant of the Rayleigh number has been taken as the difference between the hot and cold wall temperature. The maximum deviation of the correlation that takes place within the widest range has a maximum deviation of 1.41% and an average deviation of 0.67% from the real Nusselt number values presented in Tables 4 through 5. The correlations we have explored are presented in Table 6 as follows.

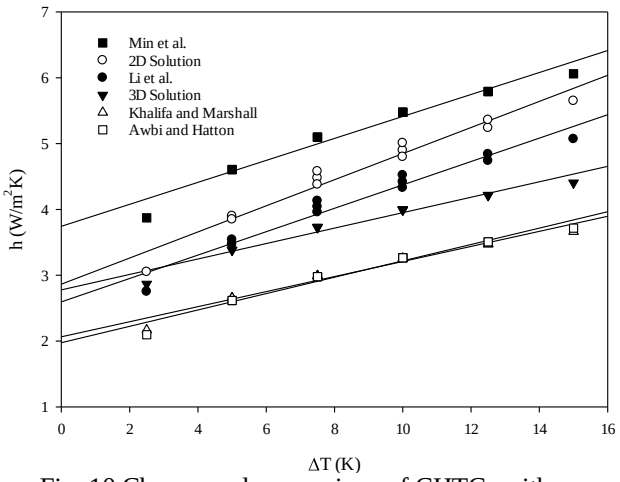

Fig. 10 Change and comparison of CHTCs with temperature difference between opposite walls for different wall temperatures (LxHxL= 1.8 x 2.85 x 1.8 m, T_c=5-15°C, T_H= 20-35°C)

The deviation of the 3-D results from the correlations derived by other researchers can be seen in Fig. 13. Despite the fact that 2-D solutions contain much more frequent meshing infrastructure, 3-D results have good agreement with Awbi and Hatton's [5] experimental study. This agreement can be clarified with "adjacent wall effects." Similar to vertical plate correlations that are shown and were used for many years in the literature, 2-D correlations also have a disadvantage. In 2-D studies, in spite of the fact that the influence of the x- and y-axis can be evaluated, the third side effect, in other words, the depth of the enclosure, cannot be taken into account in the solution period. Works in open sources illustrate that all surrounding walls in the enclosure influence the CHTCs because they have an important influence on the flow pattern. Therefore, the difference between Awbi and Hatton's [5] experimental study and the 3-D solutions of this work shows a better agreement than the 2-D solution outputs, even though 2-D solutions have a more

comprehensive meshing frequency, particularly near walls. Also, it is a general criteria in the literature that 3D solutions provide better results than those flow patterns solved by 2-D infrastructure.

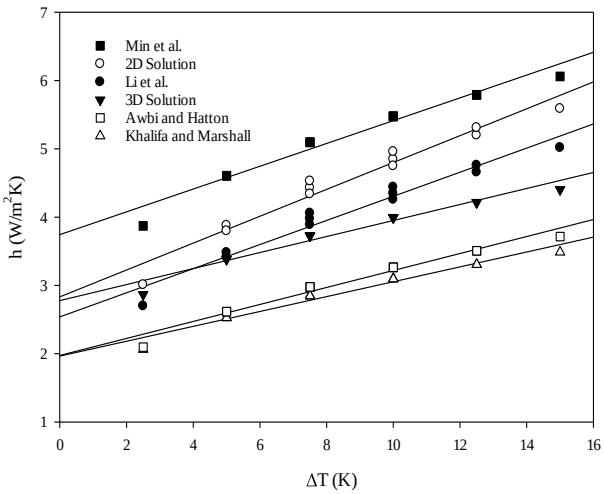

Fig. 11 Change and comparison of CHTC's with temperature difference between opposite walls for different wall temperatures (LxHxL= 4.0 x 2.85 x 4.0 m, T_c=5-15°C, T_H= 20-35°C)

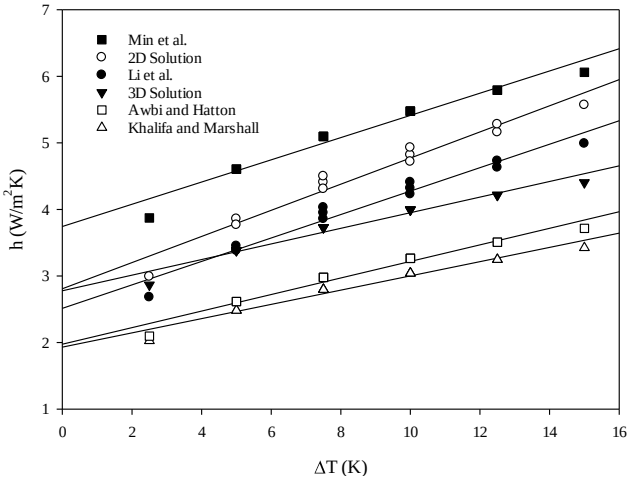

Fig. 12 Change and comparison of CHTC's with temperature difference between opposite walls for different wall temperatures (LxHxL= 6.0 x 2.85 x 6.0 m, T_c=5-15°C, T_H= 20-35°C)

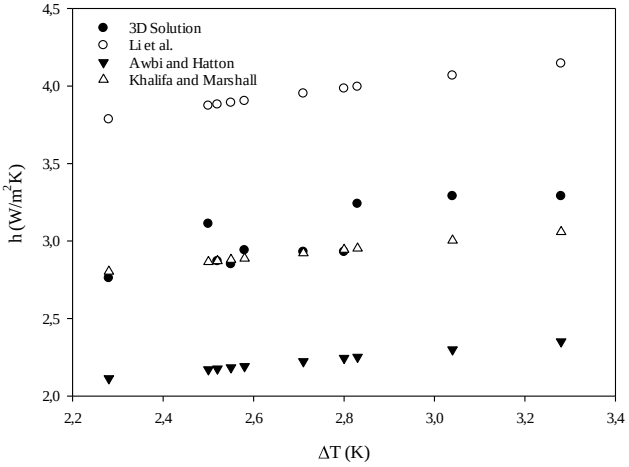

Fig. 13 Variation of CHTCs with temperature difference between hot wall and air temperatures (LxL= 1.8 x 1.8 m; H= 2.85 m; ΔT= 2.28 - 3.04)

Differences between this work and those abovementioned can be understood with the following summation: Li et. al. [14] worked in a "occupied room under normal conditions" and this situation can cause the differences. Even though Awbi and Hatton's [5] comprehensive study is the study that is the most similar to this work, they preferred "constant heat flux" (200 W/m^2) on vertical walls as boundary conditions. It is considered that this preference could bring the inconsistency between two works. The outputs have not been evaluated with correlations obtained for free plates, since it was explained that it was not suitable to evaluate free plate outputs with enclosures owing to adjacent wall effects.

The data gained through this study occurs within the range of data attained via other equations. The differences between this study and other researchers' correlation results are considered to arise from diversity within reference temperature identification, whether or not the study benefits from a 3D or 2D infrastructure, and the heat losses and gains that could not be counted by some experimental studies. Additionally, it is thought that this study's results will also be useful for the thermal comfort and energy efficiency evaluations in constructions that use hydronic radiant heating systems from walls and also depict a convenient path for building engineers in this field.

Table 6 Correlations derived within different Ra range and aspect ratios

Ra ranges	Aspect ratio (H/L)	Correlation	Max. Deviation (%)	Ave. Deviation (%)

$3.08x10^9 \le Ra_L \le 1.78x10^{10}$	1.58	$Nu_L = 0.075.(\frac{H}{L})^{0.62} Ra_L^{0.35}$	1.23	0.61
$3.38x10^{10} \le Ra_L \le 1.95x10^{11}$	0.71	$Nu_L = 0.075.(\frac{H}{L})^{-0.48} Ra_L^{0.35}$	1.31	0.54
$1.14x10^{11} \le Ra_L \le 6.59x10^{11}$	0.48	$Nu_L = 0.075.(\frac{H}{L})^{-0.48} Ra_L^{0.35}$	1.20	0.54
$3.08x10^9 \le Ra_L \le 6.59x10^{11}$	$0.48 \le H/L \le 1.58$	$Nu_L = 0.075.(\frac{H}{L})^{0.09} Ra_L^{0.36}$	1.41	0.67

III. Conclusion

This study has shown that many correlations are produced by room surfaces, particularly for heated and cooled enclosures. According to the previously published articles, discrepancies between the correlations were up to 5 for vertical surfaces of two- and three-dimensional enclosures. These differences are accounted for with scale effects, whether the heated surfaces are an insulated plate or a room surface, if radiation is taken into account, and, for experimental studies, measurement quality. The results for heated surfaces in enclosures were higher than isolated plates with free edges.

As a result of this study, via the surface and air reference temperatures that were obtained numerically, the CHTC and Nusselt numbers at a reference line in the center of the enclosure have been determined and compared with the results presented by other researchers. The results lie within the range of data derived by equations explored by other correlations. Furthermore, four correlations, while one of them valid for maximum ranges, for the Nusselt number within different Rayleigh number ranges (maximum range is $3.08x10^9 \le Ra_L \le 6.59x10^{11}$) and aspect ratios ($0.48 \le H/L \le 1.58$) have been derived including all heating, cooling (heat sink), and scale combinations that are mentioned in the text. Also, the effect of the cold wall temperature, the distance between heated and cold walls on CHTC were investigated and presented. The differences between equation outputs are considered to be affected by the reference temperature assumption, whether the study was 2-D or 3-D, and heat losses and gains that could not be counted by some experimental works.

Energy consumption and thermal comfort in buildings have tremendous impact on people's productivity, and these factors should be joined at some point. Hence, the parameters for determining heating and cooling loads in buildings should be well studied. The accurate use of CHTCs considerably influences losses from wall surfaces to the atmosphere. CHTCs are used with the conduction loss of windows while determining their total heat transfer coefficient as well. The influence of accurate use has an important effect on the total heat loss rates, as well as a great impact on thermal comfort in living spaces.

Acknowledgements

The authors are indebted to the Department of Mechanical Engineering, King Mongkut's University of Technology Thonburi (KMUTT), the Thailand Research Fund and the National Research University Project for supporting this study. Especially, the first author wishes to thank KMUTT for providing him with a Post-doctoral fellowship.

Nomenclature

C_μ, $C_{\varepsilon 1}$, $C_{\varepsilon 2}$, σ_k, σ_ε : model constants

C_p : specific heat

D : diameter (m)

G : generation of turbulence energy

H : height (m)

h : convective heat transfer coefficient, (W/m^2K)

L : length (m)

Nu : Nusselt number

p : pressure

Ra : Rayleigh number

T : temperature (K)
x,y,z : coordinates
u, v, w : velocities

Greek Letters
ρ : density, (kg/m^3)
ε : emissivity, turbulence dissipation rate
Δ : difference
μ : dynamic viscosity
μ_t : turbulent viscosity

Subscripts
C : cold
H : hot, hydrolic
k : turbulent energy

V. References

[1] ASHRAE HVAC Systems and Equipment Handbook, Chapter 6: Panel Heating and Cooling, American Society of Heating Refrigeration and Air-conditioning Engineers, USA, (2000).

[2] L. Peeters, I. Beausoleil-Morrison, A. Novoselac, Internal convective heat transfer modeling: Critical review and discussion of experimentally derived correlations. Energy and Buildings 43 (2011) 2227-2239.

[3] I. Beausoleil-Morrison, The adaptive simulation of convective heat transfer at internal building surfaces. Building and Environment 37 (2002) 791-806.

[4] S. Fohonno, G. Polidori, Modelling of natural convective heat transfer at an internal surface. Energy and Buildings 38 (2005) 548-553.

[5] H.B. Awbi, A. Hatton, Natural convention from heated room surfaces. Energy and Buildings 30 (1999) 233-244.

[6] H.B. Awbi, Calculation of convective heat transfer coefficients of room surfaces for natural convection. Energy and Buildings 28 (1998) 219-227.

[7] A.J. Khalifa, R.H. Marshall, Validation of heat transfer coefficients on interior building surfaces using a real sized indoor passive test cell. International Journal of Heat and Mass Transfer 33 (1990) 2219-36.

[8] A.J.N. Khalifa, Natural convective heat transfer coefficient a review: II. Surfaces in two- and three-dimensional enclosures. Energy Conversion and Management 42 (2001) 505-517.

[9] A.J.N. Khalifa, A.F. Khudheyer, Natural convection in partitioned enclosures: Experimental study on 14 different configurations. Energy Conversion Management 42 (2001) 653-661.

[10] A.J.N. Khalifa, Natural convective heat transfer coefficient - a review: I. Isolated vertical and horizontal surfaces. Energy Conversion Management 42 (2001) 491-504.

[11] T.C. Min, L.F. Schutrum, G.V. Parmelee, J.D. Vouris, Natural convection and radiation in a panel heated room. ASHRAE Trans 62 (1956) 337-58.

[12] R. Karadağ, The investigation of relation between radiative and convective heat transfer coefficients at the ceiling in a cooled ceiling room. Energy Conversion and Management 50 (2009) 1-5.

[13] R. Karadağ, I. Teke, H. Bulut, A numerical investigation on effects of ceiling and floor surface temperatures and room dimensions on the Nusselt number for a floor heating system. International Communications in Heat and Mass Transfer 34 (2007) 979 - 988.

[14] L.D. Li, W.A. Beckman, J.W. Mitchell, An experimental study of natural convection in an office room, large time results. Unpublished report, Solar Energy Laboratory, University of Wisconsin, Madison, 1983.

[15] M. Davies, C. Martin, M. Watson, C.N. Riain, The development of an accurate tool to determine convective heat transfer coefficients in real buildings. Energy and Buildings 37 (2005) 141-145.

[16] F.P. Incropera, D.P. DeWitt, Fundamentals of heat and mass transfer. 4th ed. New York: Wiley & Sons; 1996.
[17] http://www.fluentusers.com, accessed on 2006. Introductory FLUENT v6.3 notes.
[18] İ. Yılmaz, H.F. Öztop, Turbulence forced convection heat transfer over double forward facing step flow. International Communications in Heat and Mass Transfer 33 (2006) 508-517.
[19] O. Acikgoz, O. Kincay, Numerical determination of effects of wall temperatures on nusselt number and convective heat transfer coefficient in real-size rooms. Advances in Mechanical Engineering (2013).
[20] O. Acikgoz, AS. Dalkilic, O. Kincay, S. Wongwises, The investigation and generalization of convective heat transfer in different room geometries. Energy Technologies Conference (ENTECH14), Istanbul, Turkey, 2014.